Phys. Status Solidi B **247**, Nos. 11–12, 2855–2858 (2010) / **DOI** 10.1002/pssb.201000329

physica status solidi b
www.pss-b.com
basic solid state physics

Investigation of hydrogenated HiPCo nanotubes by infrared spectroscopy

Katalin Németh*[,1], Áron Pekker[1], Ferenc Borondics[1], Emma Jakab[2], Norbert M. Nemes[3], Katalin Kamarás[1], and Sándor Pekker[1]

[1] Research Institute for Solid State Physics and Optics, Hungarian Academy of Sciences, PO Box 49, 1525 Budapest, Hungary
[2] Institute of Materials and Environmental Chemistry, Chemical Research Center, Hungarian Academy of Sciences, P.O. Box 17, 1525 Budapest, Hungary
[3] GFMC, Departamento de Fisica Aplicada III, Universidad Complutense de Madrid, 28040 Madrid, Spain

Received 12 May 2010, revised 28 July 2010, accepted 5 August 2010
Published online 13 September 2010

Keywords carbon nanotubes, diameter selectivity, infrared spectroscopy, sidewall functionalization

* Corresponding author: e-mail nemethk@szfki.hu, Phone: +36 1 392 2222, Fax: +36 1 392 2219

Two different reductive synthetic methods were applied to hydrogenate the sidewalls of HiPCo single-walled carbon nanotubes (SWNTs). In the first one, the reductive agent was melted potassium which doped and exfoliated the nanotube bundles, so that before hydrogenation all of the tubes had been converted to metallic ones. In the second method, doping occurred just before hydrogenation by naphthalenide radical anions. The products were characterized by wide range infrared (30–52 000 cm^{-1}) spectroscopy with special emphasis on the selectivity of the two methods. We found that in the first case the controlling factor is the bandgap, and in the second case the diameter. This difference suggests the importance of the π–π interaction between naphthalenide and the nanotube surface.

1 Introduction Since 1991, the discovery of carbon nanotubes by Iijima [1], these materials have been in the focus of research. Besides their unique physical properties based on their extreme one-dimensionality, the possibility of special chemical reactions was also considered and attempted from the early days of carbon nanotube science [2].

Up to now, covalent hydrogenation of single-walled carbon nanotubes (SWNTs) was carried out by classical and modified Birch reduction [3, 4], with atomic hydrogenation by using glow-discharge [5–7], or proton bombardment [8].

We tried two different reductive methods on the nanotubes: (A) metal reduction by melted potassium, analogous to the procedure previously applied to graphite [9] and (B) reduction by naphthalenide anion produced in THF solution, both followed by reacting the tubes with methanol (Fig. 1). We are interested in the chirality-dependent changes of electronic structure and selectivity of the reactions. In order to investigate these effects, we used optical spectroscopy on the products. Optical absorption spectra are influenced by both diameter and metal/semiconductor character, therefore this method is very useful in detecting selectivity by these parameters.

Our aim was to compare the sidewall hydrogenation of HiPCo nanotubes – which have smaller average diameter and therefore higher reactivity than most of the other available carbon nanotubes [10] – by these two different methods.

2 Experimental Purified HiPCo SWNTs were from Carbon NanoTechnologies Inc. Methanol, 99.8%, sodium, and potassium were purchased from Aldrich and used as received. Toluene, 99.8% was also purchased from Aldrich and dried by vacuum cryo-distillation over K-Na alloy.

One hundred milligrams of HiPCo single-walled nanotubes – before any further process – were annealed in dynamic vacuum ($\sim 10^{-6}$ mbar) at 250 °C for 18 h in order to get rid of water and other volatile contaminants and to cure the defects in the sidewalls.

In method (A), the nanotubes were annealed with potassium in a vacuum-sealed glass vial at 200 °C for 12 h. The intercalated nanotubes were dispersed in 60 mL of anhydrous toluene in an argon dry box. One milliliter of methanol dissolved in 20 mL of anhydrous toluene was added dropwise during mild sonication. Sonication was continued for another 2 h. The mixture was filtered on a

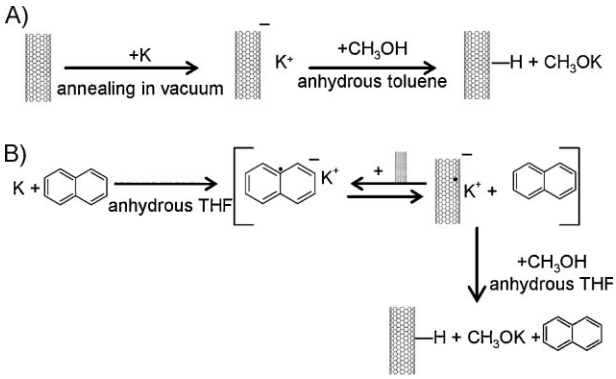

Figure 1 Reaction schemes of functionalization.

Millipore® 0.5 μm pore sized PTFE membrane, washed with methanol, distilled water, some more methanol, and dried in dynamic vacuum (200 °C, 12 h) in order to remove the residual solvents. This procedure was repeated two more times with the formerly functionalized nanotubes.

Method (B) was the one using potassium naphthalenide described in Ref. [3]. The reaction was repeated three times in this case as well.

Infrared spectra were measured with two FTIR instruments (Bruker IFS 66v/S and Bruker Tensor37) on self-supporting films, which were made by vacuum filtration [11]. Spectra were recorded between 30 and 52 000 cm^{-1}. From these wide-range spectra, we determined the optical conductivity by Kramers–Kronig transformation [12]. In the area of the transitions, we applied a baseline-correction procedure described earlier [13].

Optical conductivity is appropriate to fit with a Drude–Lorentz model. We used the fitted oscillators for background corrections. First we subtracted the contribution of the oscillators which belong to the amorphous carbon background and to the π–π^* transition. Then we assigned the remaining Lorentzians to different transitions (free carriers so-called M_{00}, S_{11}, S_{22}, *etc.*). For the analysis of a particular transition we considered the Lorentzians which do not belong to that specific transition as background and subtracted them from the spectrum. We performed this calculation for the S_{11}, S_{22}, and M_{11}-S_{33} peaks, in the latter case the different contributions were not separable. Figures 2 and 3 show the spectra related to the transitions. Each of them contains information related to only one particular set of peaks.

For Figs. 2 and 3 we consider as reference material the hydrogenated nanotube sample produced in the 1st step. We do not compare the spectra to the unreacted material (*e.g.*, after annealing at 250 °C), because many manipulations happened in the 1st step compared to this initial state, apart from the reaction, that could not be investigated by infrared spectroscopy.

3 Results and discussion According to thermogravimetry-mass spectrometry (TG-MS) measurements (not shown here), the functionalization rate of each sample is of the order of 1 mass.% of hydrogen, corresponding to one proton per 8–10 carbon atoms. The degree of functionalization increases with the number of steps in the order 1st step < 3rd step < 2nd step for reaction (A), and in the order 1st step < 2nd step < 3rd step for reaction (B). The reason for this behavior is probably an equilibrium process which will be discussed elsewhere.

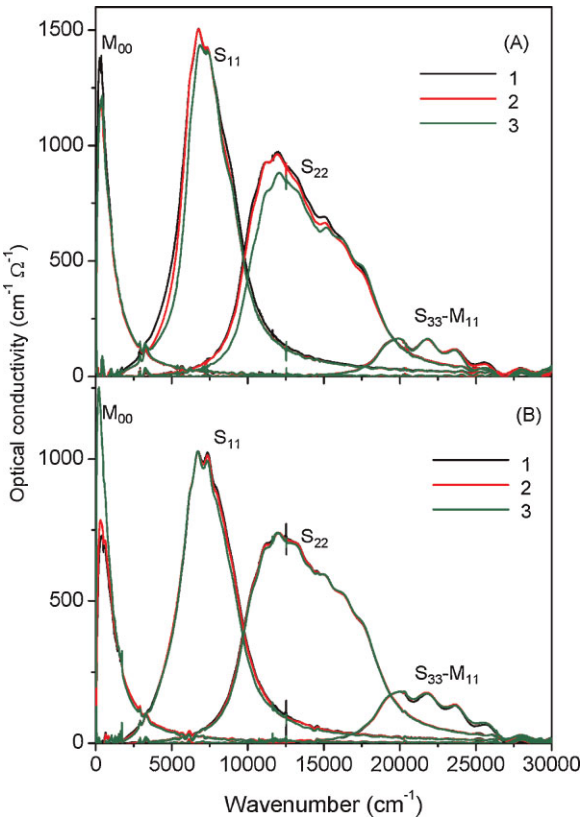

Figure 2 (online color at: www.pss-b.com) Baseline-corrected optical conductivity of functionalized HiPCo nanotubes. Upper: samples made by reaction (A); lower: made by reaction (B). Curves 1,2, and 3 correspond to increasing order in the degree of functionalization.

The optical conductivity of the functionalized nanotubes in selected regions of the spectrum is shown in Figs. 2 and 3. The changes are slight, according to the low degree of functionalization, but there are distinct differences between the products obtained by the two reaction types.

The decrease in optical conductivity upon functionalization at the transitions between Van Hove singularities is caused by the transformation of sp^2 into sp^3 carbon atoms. We observe that this decrease is not uniform and depends on the reaction mechanism: for reaction type (A), the low-energy part is decreasing faster, while for reaction type (B), the opposite happens. The effect is visible for both S_{11} and S_{22} transitions (Fig. 2). In Fig. 3 we enlarged the S_{11} region (6000–8500 cm^{-1}) and illustrate the changes on these transitions.

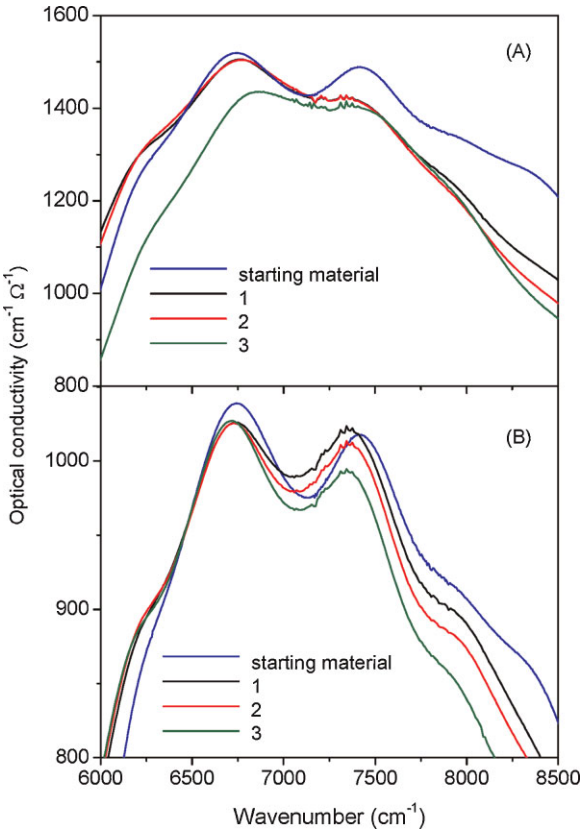

Figure 3 (online color at: www.pss-b.com) Region of S_{11} transitions enlarged. Upper: reaction (A); lower: reaction (B). Curves 1,2, and 3 correspond to increasing order in the degree of functionalization. Starting material is the HiPCo annealed at 250 °C for 18 h.

The peak in the conductivity shown in Fig. 3 is a convolution of the S_{11} transitions of many semiconducting nanotubes, in the order of increasing gap energy. Since the gap energy is inversely proportional to the tube diameter, smaller tubes cause intensity at higher frequencies. The message of Fig. 3 is thus that reaction (A) favors larger diameter (smaller gap) tubes, and reaction (B) is more selective toward small diameter tubes.

This difference is somewhat surprising, since the underlying mechanism is thought to be similar, a charge transfer from an electron donor resulting in excess electron density of the nanotube, followed by a reaction of the carbanions with the respective alcohol [3]. Chemical arguments, based on π-orbital misalignment [10], would dictate that nanotubes with larger curvature, *i.e.*, smaller diameter, should be more sensitive toward sidewall functionalization. This is clearly the case in reaction type (B), but not in reaction type (A).

The two reaction types differ in the details of the charge transfer step. In reaction (A), potassium metal, a strong electron donor is applied in large excess, resulting in delocalized electrons on the nanotubes and potassium ions intercalated inside nanotube bundles. In this case, the conduction bands of the nanotubes will be filled with electrons in the order of increasing gap, which means reverse order of diameter. The more doped the tubes are, the higher the reaction rate in the second step.

In reaction (B), the electron donor is the naphthalenide molecular ion, a planar aromatic system which can enter into π–π interaction with the nanotube surface [14]. Such contact may lead to localized carbanion sites, and the production of such sites can depend on the curvature. Since the localized excess electron reduces local strain caused by curvature, the energy gain is larger on smaller diameter tubes.

The two reaction types differ in the details of the charge transfer step. In reaction (A), potassium metal, a strong electron donor is applied in large excess, resulting in delocalized electrons on the nanotubes and potassium ions intercalated inside nanotube bundles. In this case, the conduction bands of the nanotubes will be filled with electrons in the order of increasing gap, which means reverse order of diameter. The more doped the tubes are, the higher the reaction rate in the second step.

In reaction (B), the electron donor is the naphthalenide molecular ion, a planar aromatic system which can enter into π–π interaction with the nanotube surface [14]. Such contact may lead to localized carbanion sites, and the production of such sites can depend on the curvature. Since the localized excess electron reduces local strain caused by curvature, the energy gain is larger on smaller diameter tubes.

In the M_{11} region, there is no apparent change with degree of functionalization, indicating selectivity of both reactions toward semiconducting nanotubes. The increase in the free-carrier Drude peak (M_{00}) in the third step of reaction (B) merits further investigation, but can be caused by extrinsic doping effects as well.

4 Conclusions We applied two different reductive methods for hydrogenation of HiPCo SWNTs with different mechanisms and investigated the effect of mechanism on the distribution of the products. According to wide-range infrared spectra, from S_{11} peaks we concluded that in the first case, when the reactivity is determined by doped tubes with delocalized charge carriers, the larger diameter tubes react first. In the second one, where the dopant enters into non-covalent chemical interaction with the tube surface and localized carbanions are formed, reactivity is determined by curvature and smaller diameter tubes are favored.

Acknowledgements This work was supported by the Hungarian Scientific Research Fund OTKA NKTH under grant nos. 72954, 67842, and 75813.

References

[1] S. Iijima, Nature **354**, 56 (1991).
[2] D. Tasis, N. Tagmatarchis, A. Bianco, and M. Prato, Chem. Rev. **106**, 1105 (2006).
[3] F. Borondics, E. Jakab, and S. Pekker, J. Nanosci. Nanotechnol. **7**, 1 (2007).
[4] S. Pekker, J.-P. Salvetat, E. Jakab, J.-M. Bonard, and L. Forró, J. Phys. Chem. B **105**, 7938 (2001).

[5] B. N. Khare, M. Meyyappan, A. M. Cassell, C. V. Nguyen, and J. Han, Nano Lett. **2**, 73 (2002).
[6] B. N. Khare, M. Meyyappan, J. Kralj, P. Wilhite, M. Sisay, H. Imanaka, J. Koenhe, and C. W. Baushchlicher, Appl. Phys. Lett. **81**, 5237 (2002).
[7] K. S. Kim, D. J. Bae, J. R. Kim, K. A. Park, S. C. Lin, J. J. Kim, W. B. Choi, C. Y. Park, and Y. H. Lee, Adv. Mater. **14**, 1818 (2002).
[8] B. N. Khare, M. Meyyappan, M. H. Moore, P. Wilhite, H. Imanaka, and B. Chen, Nano Lett. **3**, 643 (2003).
[9] D. E. Bergbreiter and J. M. Killough, J. Am. Chem. Soc. **100**, 2126 (1978).
[10] S. Niyogi, M. A. Hamon, H. Hu, B. Zhao, P. Bhowmik, R. Sen, M. E. Itkis, and R. C. Haddon, Acc. Chem. Res. **35**, 1105 (2002).
[11] Z. Wu, Z. Chen, X. Du, J. M. Logan, J. Sippel, M. Nikolou, K. Kamaras, J. R. Reynolds, D. B. Tanner, A. F. Hebard, and A. G. Rinzler, Science **305**, 1273 (2004).
[12] Á. Pekker, F. Borondics, K. Kamarás, A. G. Rinzler, and D. B. Tanner, Phys. Status Solidi B **243**, 3485 (2006).
[13] Á. Pekker, D. Wunderlich, K. Kamarás, and A. Hirsch, Phys. Status Solidi B **245**, (1954). (2008.
[14] H. Ulbricht, R. Zacharia, N. Cindir, and T. Hertel, Carbon **44**, 2931 (2006).

